www.elsevier.com/locate/yjtbi

A Nutrient Dependant Switch Explains Mutually Exclusive Existence of Meiosis and Mitosis Initiation in Budding Yeast

C.T. Wannige, D. Kulasiri, S. Samarasinghe

PII: S0022-5193(13)00466-9
DOI: http://dx.doi.org/10.1016/j.jtbi.2013.09.030
Reference: YJTBI7475

To appear in: *Journal of Theoretical Biology*

Received date: 13 August 2013
Accepted date: 20 September 2013

Cite this article as: C.T. Wannige, D. Kulasiri, S. Samarasinghe, A Nutrient Dependant Switch Explains Mutually Exclusive Existence of Meiosis and Mitosis Initiation in Budding Yeast, *Journal of Theoretical Biology,* http://dx.doi.org/10.1016/j.jtbi.2013.09.030

A Nutrient Dependant Switch Explains Mutually Exclusive Existence of Meiosis and Mitosis Initiation in Budding Yeast

C. T. Wannige[1], D. Kulasiri*[1], S. Samarasinghe[1]

1. Centre for Advanced Computational Solutions (C-fACS), Department of Molecular Biosciences, Lincoln University, Christchurch, New Zealand

*corresponding Author : Don Kulasiri, Centre for Advanced Computational Solutions (C-fACS), Department of Molecular Biosciences, Lincoln University, Christchurch, New Zealand.

Tel: + 64 3 325 2811 E-mail: don.kulasiri@lincoln.ac.nz

Funding: The authors received no specific funding for this study.

Abstract

Nutrients from living environment are vital for the survival and growth of any organism. Budding yeast diploid cells decide to grow by mitosis type cell division or decide to create unique, stress resistant spores by meiosis type cell division depending on the available nutrient conditions. To gain a molecular systems level understanding of the nutrient dependant switching between meiosis and mitosis initiation in diploid cells of budding yeast, we develop a theoretical model based on ordinary differential equations (ODEs) including the mitosis initiator and its relations to budding yeast meiosis initiation network. Our model accurately and qualitatively predicts the experimentally revealed temporal variations of related proteins under different nutrient conditions as well as the diverse mutant studies related to meiosis and mitosis initiation. Using this model, we show how the meiosis and mitosis initiators form an all-or-none type bistable switch in response to available nutrient level (mainly nitrogen). The transitions to and from meiosis or mitosis initiation states occur via saddle node bifurcation. This bidirectional switch helps the optimal usage of available nutrients and explains the mutually exclusive existence of meiosis and mitosis pathways.

***Key words*:** Bistable switching; Negative-feedback; Bifurcation; *Saccharomyces cerevisiae*

Authors' contributions: The first and second authors developed the conceptual and mathematical models; the first author did all the computational work; the third author contributed to the data analysis, parameter estimation and clarifications related to the cell cycle; the first and second author wrote the paper with third author's assistance.

1. Introduction

Molecular mechanisms have been fined-tuned through natural selection over millennia of evolution for survival and growth of organisms under varying nutritional conditions. For example, when deprived of nutrients, each grown, diploid budding yeast (*Saccharomyces cerevisiae*) cell survives by switching to meiosis type cell division creating four unique

stress-resistant spores (Morgan, 2006). Conversely, in good nutritional conditions, each grown cell contributes to the growth of the organism by switching to mitosis type cell division creating two exactly similar daughter cells (Gupta, 2009). Recent research provide an in-depth process level understanding of the regulation of budding yeast meiosis and mitosis cell division including their temporal, sequential gene regulation and component wise feedback control at the extreme nutrient conditions (abundance or starvation): abundance initiates mitosis whereas starvation triggers meiosis (Barik et al., 2010; Gurevich et al., 2010; Kaizu et al., 2010; Nachman et al., 2007; Piekarska et al., 2010). Budding yeast cells can choose between meiosis or mitosis initiation alternatively according to the available nutrients until an irreversible point called 'commitment point'(Simchen, 2009). In this paper, we investigate the systemic behaviour of nutrient dependant meiotic-mitotic switching between these two pathways using mathematical modelling.

The diploid yeast cells decide to undergo different development pathways, such as meiosis or mitosis (Fig. 1), depending on environmental conditions at the START check point of the G1 phase of cell cycle (Forsburg and Nurse, 1991). The protein complex, Cdk1/Cln3[1] is the most upstream activator of the START checkpoint, and it is identified as the G1 specific transcriptional activator of budding yeast mitosis (de Bruin et al., 2004; Gallego et al., 1997); high concentration of Cdk1/Cln3 allows traversing through G1 to S phase of the cell cycle in mitosis [22]. When the low levels of Cdk1/Cln3 do not promote entry into the cell cycle, *high levels* of proteins Ime1 and Ime2, the two principal regulators of meiosis initiation, trigger meiosis in nutritionally stressed conditions, resulting in G1 arrest (Pnueli et al., 2004). In contrast, IME1 mRNA low basal levels and Ime2 undetectable levels are found in the nutritionally rich, mitotic conditions (Shenhar and Kassir, 2001). Kassir et al. (Gurevich et al., 2010) experimentally observed a double negative feedback loop, a major component of a bistable switch, between meiosis and mitosis initiators (Ime2 and Cdk1/Cln3). Motivated by these experimental studies, to understand the behaviour of the nutrient dependant switch, we incorporate the protein network which includes both the meiosis and mitosis initiators and their main regulators (Fig. 2) in modelling.

Mathematical modelling has been used to understand the machinery of mitosis cell cycle at high nutrients (Chen et al., 2000; Chen et al., 2004; Vinod et al., 2011), and these studies are helpful for the understanding of the human cell cycle, as the molecular mechanisms are

[1] Notation : Protein names are written in lower case starting with an uppercase letter, and genes and mRNAs are written in upper case.

conserved in human and yeast cell cycles (Kaizu et al., 2010). The available deterministic models can be categorised into two groups depending on their objectives: (1) cell cycle regulation focussed models, where the cell cycle is modelled and controlling mechanisms at checkpoints such as START, G1/S are studied by analysis (Barik et al., 2010; Tóth et al., 2007; Verdugo et al.; Vinod et al., 2011); and (2) cell cycle's temporal organisation focussed models, which explain orderly progression of the cell cycle steps by the periodical activation and inactivation of the associated regulators (mainly Cdks and Cyclins) (Chen et al., 2004; Hong et al., 2012; Tyson and Novak, 2008).

Comparably, there are fewer mathematical studies of meiosis (Ray et al., 2013; Rubinstein et al., 2007; Shen et al., 2010) than mitosis in the literature; and among them, two mathematical models (Ray et al., 2013; Rubinstein et al., 2007) have been proposed to describe meiosis initiation. The most common feature of these two modelling studies is that both of them investigate the feedback loops involved in meiotic initiation. The model developed by Rubinstein et al., (2007) is a Boolean network of meiosis initiation of budding yeast, which includes main initiator proteins, Ime1 and Ime2, their regulators, Ume6 and Rpd3, and two putative nodes representing the negative regulation of Ime1 and Ime2. (The model is a discrete transition system representing the initiation process by a graph whose nodes represent RNA or proteins, and the edges denote regulation.) This model explains the qualitative behaviour of meiosis initiation including the transient and sequential expression patterns of meiotic inducers at nutrient starved conditions and they have interrogated the model to explore variations to their basic network to identify the negative feedback loops that affect the transcription of meiosis initiators. However, the model restricts the protein/RNA expression level to a maximum value of nine which limits the protein and mRNA expression only to that threshold cutting off further expression (Fig. 2A and Fig.3A in (Rubinstein et al., 2007)). Further, the weights for each edge are decided without considering the actual mechanisms and do not provide a detailed representation hindering the model's predictive capability. In ensuing years new experimental studies revealed new interactions among the components of the initiation process: meiosis initiators and Cdk1/Cln3(Gurevich et al., 2010; Holt et al., 2007; Szwarcwort-Cohen et al., 2010), and negative regulators of IME1 transcription and Ime2 transient transcription (Rubinstein et al., 2007).

Ray et. al.(Ray et al., 2013) developed an ODEs based model for yeast sporulation which is the most recent mathematical model. This model, which only includes Ime1, Ime2, Rim11, Ume6, Sok2 and the feedback loops between them simulates the orderly and transient

dynamics of meiotic initiators. The model is validated using quantitative phenotypes of single gene knockouts. Similar to the first Boolean network model, this model investigates the effects of feedback loops for meiosis initiation and predicts that both positive and negative feedback loops are essential for the transient expression of meiotic regulators; for example, auto-positive feedback loop of Ime2 is required for its transient expression. The model is an abstraction of pathway incorporating components and the effects of other molecules are reflected indirectly: double negative feedback loop between Ime2, Cdk1/Cln3 and mutual activation between Ime2, Ndt80 are both captured by auto-regulation of Ime2; Cdk1/Cln3, Msn2/4, Snf1 are collectively represented by an activation signal. Some important well researched participants and connections such as Nitrogen involvement in Ime1 expression initiation, and Rpd3/Sin3 involvement in EMG repression are not considered in this model. The model predicts that the Ime1 and Ime2 expressions are transient, but Ime2 maximum level is higher than that of Ime1 contradicting the previously published extended Boolean network outputs and experimental mRNA levels (Fig.2 of (Rubinstein et al., 2007)). Further, the model is not validated with the available experimental data of the temporal behaviour of the Ime1 and Ime2 protein expressions (Nachman et al., 2007; Shefer-Vaida et al., 1995).

Both of the aforementioned models examine the meiosis initiation network structure, especially the feedback loops, at low nutrient conditions. To date, there are no available models which explore the initial meiotic-mitotic switching behaviour in budding yeast in different nutrient conditions. In this study, we explore the initial meiotic-mitotic switching dynamics by extending the Boolean model (Rubinstein et al., 2007), which is more biologically sound with stronger experimental validity than the second, and by including recent findings. We develop the model in an ODE framework enabling us to perform phase plane and bifurcation analyses to obtain deeper insights into the system behaviours.

The structure of the paper is as follows: a brief description of molecular biology of meiosis and mitosis initiation is given in Section 2; the new model development and validation is discussed in Section 3; The main findings from the model is presented in the Section 4; finally, the biological insights obtained from the modelling are discussed in Section 5.

2. Biology of budding yeast meiosis and mitosis initiation

In this section, we succinctly review the specific details of meiosis, mitosis initiation and nutritional dependence of budding yeast cells. (Readers are referred to (Harvey Lodish, 1995; Morgan, 2006) for in-depth review of the subject.)

The model eukaryote, budding yeast *Saccharomyces cerevisiae*, can stably exist either as diploid cells, which have two sets of chromosomes, or haploid cells, which have a single set of chromosomes. In yeast cells, meiosis or mitosis cell division initiation decision depends on nutritional conditions and cell size: Meiosis and mitosis initiate at opposite nutritional conditions (Fig. 1). Meiosis initiates in grown, diploid yeast cells in nutritional stress or meiotic conditions: acetate medium with limited or no nitrogen and in the absence of glucose (Burgess et al., 1999; Kassir et al., 2003). In contrast, mitosis initiates in both haploid and diploid cells in good nitrogen and carbon conditions (mainly glucose), called vegetative conditions (Morgan, 2006).

Meiosis process consists of a gene cascade with three major sets, which are expressed sequentially: Early (EMG), Middle (MMG) and Late (LMG) meiosis specific genes. IME1(Initiator of Meiosis1), which is activated and regulated mainly by nitrogen, is responsible for activating EMGs including IME2(Initiator of Meiosis2) (Kassir et al., 2003). Upon nutritional stress, the EMG repressor complex Rpd3/Sin3 (histone deacetylace) on the DNA binding protein Ume6 is partially replaced by Ime1 in the following manner: active Rim15 kinase phosphorylates Ume6, and Sin3 (see Fig 9 of (Pnueli et al., 2004)); as a result, Ume6 disassociates from Sin3 and removes Rpd3/Sin3 from the EMG promoters; at the same time, the kinase active Rim11 phosphorylates Ime1, and this is required to relieve the Rpd3 repression and to enable the interaction of Ime1 with Ume6. The mechanism of the removal of the other IME2 repressor complex Isw2 (chromatin remodelling complex) is unclear (Kassir et al., 2003). Ime2 is a positive regulator of MMG and LMG transcription, and it is required for the efficient transcription of all EMGs (Morgan, 2006). Both Ime1 and Ime2 possess positive autoregulation. Recent research show that IME1 expression is repressed by Rpd3S complex (Rubinstein et al., 2007). Further, Ime2 phosphorylates Ime1 thereby tagging for degradation (Kassir et al., 2003). MMGs, which are responsible for nuclear divisions and spore formation, activate LMGs responsible for spore maturation (Gurevich et al., 2010).

Mitotic cell cycle is driven by the Cyclins which activate Cyclin dependent kinases (Cdks) (Gupta, 2009; Morgan, 2006). The most upstream activator, Cln3's mRNA levels are

positively regulated by nitrogen and glucose (Parviz and Heideman, 1998). Increased Cdk1/Cln3 levels stimulate further downstream mitotic genes upon vegetative conditions (Gallego et al., 1997; Gupta, 2009). However, Cln3 is reduced mainly by transcriptional repression, translational repression and degradation upon nitrogen depletion (Colomina et al., 1999; Gallego et al., 1997; Parviz and Heideman, 1998). Experiments recently revealed a double negative feedback loop between Ime2 and Cdk1/Cln3 (Gurevich et al., 2010; Holt et al., 2007; Szwarcwort-Cohen et al., 2010). Additionally, Cln3 phosphorylates and transports Ime1 out of the nucleus (Kassir et al., 2003) and, Cln3 transcriptionally represses IME1(Colomina et al., 1999).

3 Development of the new model

3.1 Assumptions of the model

The model we propose (Fig. 2) consists of main meiosis and mitosis initiators (Ime1, Ime2, Cdk1/Cln3), their repressors/activators (Rpd3/Sin3, Rpd3S) and regulators (Nitrogen, Rim15). Biologically meaningful assumptions allow us to present the information at a higher level of abstraction which would encapsulate the essential mechanisms.

We assume that all the participating reactions take place in a single compartment, as meiosis and mitosis initiation can be considered as nuclear events (Kassir et al., 2003). Most of the transcriptional initiators, including Ime1 and Ime2, are localised to the nucleus of the yeast cell during meiosis initiation (Kominami et al., 1993; Pnueli et al., 2004). Even though the translation of mRNA happens at the cytoplasm and meiosis related nutritional signals arrive from outside of the plasma membrane through the cytoplasm to the nucleus, most of the meiosis related reactions happen inside the nucleus (Kassir et al., 2003). This assumption is the basis of modelling the system as a single compartment and the molecular transport times are ignored. We mainly focus on the nutritional dependence of meiosis and mitosis initiation in grown diploid yeast cells. Therefore, the model is valid only for grown diploid yeast cells, and we do not consider the cell type and size control in meiosis and mitosis initiation.

The nutrition affecting meiosis and mitosis initiation includes nitrogen, glucose and non-fermentable carbon sources such as acetate. Among all the other nutrients, nitrogen plays a major role in meiosis and mitosis initiation regulation (Figure 1 of (Kassir et al.,

2003),(Gurevich et al., 2010)). Furthermore, glucose plays a parallel role to nitrogen in meiosis and mitosis initiation (low glucose helps meiosis initiation and high glucose helps mitosis similar to nitrogen) (Parviz and Heideman, 1998; Pnueli et al., 2004). Therefore, we focus only on the effects of nitrogen on meiosis and mitosis initiation, and we assume glucose and other nutrients are available in appropriate amounts.

Under vegetative conditions, the EMGs including IME2 are repressed by Isw2 and Rpd3/Sin3. As the mechanism of Isw2 removal is not known (Kassir et al., 2003), it is assumed that Isw2 is removed from the promoters in a parallel way to Rpd3 and its involvement in repression is not considered in the model.

We include the recent research finding of double negative feedback loop between Ime2 and Cdk1/Cln3 to our model, since this relation would affect the switching dynamics. In one of the negative feedback loops between Ime2 and Cdk1/Cln3, functionality of Cdk1 is inhibited by Ime2, because probably all known substrates of Cdk1 are phosphorylated by Ime2 inhibiting the cell cycle progression (Holt et al., 2007; Szwarcwort-Cohen et al., 2009). Further, Cdk1 phosphorylates and tags Cln3 for degradation (Szwarcwort-Cohen et al., 2010). As Cdk1 substrates are not included in our model, we assume that Ime2 phosphorylates Cdk1/Cln3 and perturbs its functionality.

Ime2 functionality is inhibited in the other negative feedback loop between Ime2 and Cdk1/Cln3; three phosphorylation sites exist in Ime2 where Cak1 and Cdk1 can bind to and phosphorylate Ime2. Cak1 phosphorylation activates Ime2. Cdk1 phosphorylates Ime2 at the same sites where Cak1 binds for phosphorylation (Schindler et al., 2003). For simplicity, the involvement of Cak1 is not considered in this model; instead, it is assumed that Ime2 activates itself, and its activity is inhibited by the Cdk1 phosphorylation. In this model we ignore the mediator, Ume6 on EMG promoters, and assume direct and simultaneous binding of Rpd3/Sin3 and Ime1 to EMGs.

As mentioned in Section 2, upon Nitrogen depletion, active Rim15 phosphorylates Ume6 and Sin3 thereby breaking the relationship between the Ume6 and Rpd3/Sin3 complex. We assume the relief of Rpd3 on EMG promoter is proportional to the active Rim15 amount. Upon transformation to meiotic medium, RIM15 is not transcribed, and Rim15 protein gradually disappears (Pnueli et al., 2004). Since RIM15 gene regulation is unclear, we model active Rim15 protein as a decreasing function from its maximum expression level, which depend on the available nitrogen level, to a minimum level (Fig. 4). According to this

assumption, at the top level, active Rim15 degrades Rpd3/Sin3 complex on EMG promoters. Further, Rim11 phosphorylates Ime1, which then represses Rpd3/Sin3 complex. For simplicity, it is assumed that Ime1 directly degrades Rpd3/Sin3. Further, it is assumed that the degradation of Ime1 also directly depends on Ime2 as Ime2 phosphorylates and tags Ime1 for degradation. We ignore the phosphorylations and de-phosphorylations associated with Rim11, Rim15 and Ime1 which implies that they are faster reactions, and the magnitude of reaction rates are such that by ignoring these reactions the system dynamics would not change significantly.

According to the assumption of nuclear localisation of reactions, the phosphorylated Ime1 by Cln3 is degraded inside the nucleus rather than its actual transportation out of the nucleus. The Cdk1 expression in budding yeast is constant, and the stability, activity and the expression of Cyclins are regulated during the cell cycle (Miller and Cross, 2001; Pramila et al., 2002). Therefore, it is assumed that the active Cdk1/Cln3 amount depends on Cln3 level. Further, Cdk1 is assumed to have a higher level of relative abundance than Cln3.

Typical meiosis initiation conditions include low basal level of Ime1 and high level of Rpd3/Sin3 (Rubinstein et al., 2007). The initial and maximum protein concentrations are calculated as follows: the ellipsoidal budding yeast cells have a large diameter of 5-10 μm and a small diameter of 1-7μm (Schaechter, 2011). Assuming the nucleus radius of length as 3.75μm, width as 2.5μm and height as 2μm, volume of an ellipsoid is V=4/3*radius of length* radius of width* radius of height = 7.85×10^{-14} L =7.85×10^{-17} m^3. The number of molecules corresponding to 1nM is (7.85×10^{-17} m^3) × (10^{-6} mole/m^3) × (6×10^{23} molecules/mole) = 47 molecules. The Ime2 protein abundance in rich medium is 538 molecules per cell (Lu et al., 2006), and this number is assumed as the basal level of each proteins in our model (10-11nM). As the maximum Ime1 protein expression level is around relative levels of 6 and 7 (β-gal units: 60 and 70) in (Shefer-Vaida et al., 1995), the maximum protein level is then approximately 100nM. Considering the maximum Ime1 protein expression relative level of 6 (Shefer-Vaida et al., 1995), and as the experiments revealed that Rpd3/Sin3 is at its maximum activity at early stage (Pnueli et al., 2004; Rubinstein et al., 2007), initial condition for Rpd3/Sin3 is decided as 60nM (6 times from the basal level). According to the experimental levels of Cln3 expression (Fig. 7 of (Gallego et al., 1997)) the basal level of Cln3 is also assumed as the basal level of 10nM. Later, we non-dimentionalize these concentrations so that the maximum expression level is 1 (corresponds to 100nM), and

minimum is 0 in order to compare the model variables with the corresponding experimental variables.

3.2 Equations of the model

Considering the time dependence of each component, the relations in the schematic diagram (Fig. 2) are converted into an ODE model, describing the rate of synthesis and degradation.

Protein synthesis rate is modelled as a function of transcription factor concentrations. Although these protein synthesis functions ignore mRNA level information, it is commonly used in systems biology modelling where protein synthesis patterns show similarities to their mRNA expression (Mehta et al., 2008; Novak and Tyson, 2004; Rosenfeld et al., 2005; Süel et al., 2006). We used this approach for protein synthesis functions, considering the similarities between the mRNA and protein expression levels of meiosis initiators, and the negligible nucleo-cytoplasmic transportation delay compared with the meiosis initiation time frame (The typical mRNA transcription time of *S.cerevisiae* is about 1 minute including mRNA pre-processing time. The time to translate a protein takes about 2 minutes including the nucleo-cytoplasmic transportation delay (Alon, 2007). Comparably, meiosis initiation time frame is longer and about 20-25 hours (Rubinstein et al., 2007)).

Equation (1) represents the temporal variation of active Ime1.

$$\frac{dfIme1}{dt} = \alpha_{fIme1} + \beta_{fIme1} \left[\left(\frac{fIme1^{n1}}{K_{fIme11}{}^{n1} + fIme1^{n1}} \right) \left(\frac{K_{N_2}^{n_2}}{K_{N_2}^{n_2} + N_2^{n_2}} \right) \left(\frac{K_{Rpd3SIme1}^{n_{11}}}{K_{Rpd3SIme1}^{n_{11}} + \left(Rpd3S\right)^{n_{11}}} \right) \left(\frac{K_{Cdk1/Cln3}^{n_9}}{K_{Cdk1\backslash Cln3}^{n_9} + Cdk1\backslash Cln3^{n_9}} \right) \right] - \gamma_{PIme1Cln3} \left(\frac{Cdk1\backslash Cln3^{n_{10}}}{Cdk1\backslash Cln3^{n_{10}} + K_{PIme1Cdk1\backslash Cln3}^{n_{10}}} \right) - d_{fIme1} \left(fIme2\right)(fIme1) \quad (1)$$

$$Rpd3S = \left(n_{12} - \left(n_{12} \left(1 - exp\left(t - 6 \right) \right) \right) \right)$$

The first term (α_{fIme1}) on the right hand side (r.h.s) is the basal synthesis rate of Ime1 when the auto regulation, nitrogen, Rpd3S and Cln3 repression are not occurring. The second term describes the protein synthesis rate as a function of Nitrogen, Cln3, Rpd3S and Ime1 transcription factor concentrations. Hill functions are used to model transcriptional activation, repression and phosphorylation assuming these processes are ligand-receptor binding and

unbinding reactions (Angeli et al., 2004; Dushek et al., 2011; Zi et al., 2010). Rpd3S gene expression is unclear. Therefore, we model the Rpd3S level as a sigmoid increasing function (Equation 1.1 and Fig. 3) as in the extended Boolean model of meiosis initiation (Rubinstein et al., 2007). The third term describes phosphorylation of Ime1 by Cln3 and the transportation of phosphorylated Ime1 out of the nucleus which is assumed as degradation. The last term represents the Ime1 protein degradation by itself and with the help of Ime2.

The following equation describes the rate of change of active Ime2 protein:

$$\frac{dfIme2}{dt} = \alpha_{fIme2} + \beta_{fIme2} \left[\left(\frac{fIme2^{n_3}}{K_{fIme22}^{n_3} + fIme2^{n_3}} \right) \left(\frac{fIme1^{n_4}}{K_{fIme12}^{n_4} + fIme1^{n_4}} \right) \left(\frac{K_{Rpd3/Sin3}^{n_5}}{K_{Rpd3\backslash Sin3}^{n_5} + Rpd3 \backslash Sin3^{n_5}} \right) \right] - \gamma_{PIme2} \left(\frac{Cdk1 \backslash Cln3^{n_6}}{Cdk1 \backslash Cln3^{n_6} + K_p^{n_6}} \right) - d_{fIme2} \left(fIme2 \right) \quad (2)$$

The first term on the r.h.s. of the equation (2) is the basal synthesis rate of Ime2 protein. IME2 expression is repressed by Rpd3/Sin3 complex and activated by Ime1. IME2 is auto activated similarly as IME1. As it is assumed that the Ume6 is not involved in repression and Ime1 activation, they are directly modelled by using Hill functions in the second term. Third tem represents the deactivation of Ime2 by Cdk1/Cln3 phosphorylation by a Hill function. Fourth term represents the normal self-degradation of Ime2 protein.

Third equation corresponds to the variation of active Cdk1/Cln3 with time:

$$\frac{dCdk1 \backslash Cln3}{dt} = \alpha_{Cln3} + \beta_{Cdk1CLn3} \left(\frac{N_2^{n_7}}{K_{N_{2Cln3}}^{n_7} + N_2^{n_7}} \right) - \gamma_{PCdk1Cln3} \left(\frac{fIme2^{n_8}}{K_{PIme2Cdk1}^{n_8} + fIme2^{n8}} \right) - d_{Cln3} \left(Cdk1 \backslash Cln3 \right) \quad (3)$$

As Cdk1 protein is assumed to be constantly abundant and as its activation depends on Cln3, the expression rate of active Cdk1/Cln3 depends on the nitrogen activation only. The first term on the r.h.s represents the basal expression rate, and the second term models the

activation of Cln3 expression by a Hill type function. According to the assumption that Cdk1/Cln3 can be inactivated by the phosphorylation of Ime2, this phosphorylation relationship is modelled with a Hill type function. It is subtracted as it inactivates Cdk1/Cln3 functionality. Last term represents the self-degradation of Cdk1/Cln3.

Fourth equation describes the temporal variation of Rpd3/Sin3 complex on EMG promoter:

$$\frac{dRpd3\setminus Sin3}{dt} = \alpha_{Rpd3Sin3} - d_{Rpd3Sin3}\, fIme1\, Rim15 \tag{4}$$

$$Rim15 = \frac{1}{N_2}\left(\frac{n_{13}}{n_{15} + \exp(1.6t)} + n_{14}\right) \tag{}$$

The first term on r.h.s. describes the formation rate of Rpd3/Sin3 complex. As mentioned in section 3.1, the separation of Rpd3/Sin3 from Ume6 is simplified and assumed that the Rpd3/Sin3 complex is degraded proportional to the available Ime1 and Rim15 amount. Rim15 term represents the related relief of Rpd3/Sin3, which depends on the active Rim15 amount. Since RIM15 gene regulation is unclear, we model active Rim15 protein as a decreasing function from the maximum expression level (depending on the available nitrogen level) to minimum (Equation 4.1) as shown in Fig. 4 using the following available facts: Upon transformation to meiotic medium, RIM15 is not transcribed and Rim15 protein degrades and disappears (Fig. 4 A) (Pnueli et al., 2004); In good nutrients Rim15 is unavailable as it is inactivated by phosphorylation (Fig. 4 B).

We partially non-dimentionalized our model using the total protein levels (Table A.1 of Appendix A) (De Vries, 2006), as this approach reduces the complexity of our model; and, the results can be compared with the available experimental, relative concentration levels. In non-dimentionalization, the fraction of protein level to the total amount was used instead of the absolute protein values. The non-dimentionalized model was numerically solved by using the 'Ode45s' function in Mathlab R2010a (The Mathworks, Natick, MA, and U.S.A).

3.3 Parameter Estimation

We use experimentally measured value ranges to determine the specific set of parameters given in Table 1. When the whole range of a parameter is unavailable, the available parameter values are allowed to vary 50 times from the highest reference experimental value and one fiftieth from the lowest reference value to cover experimental error and cellular heterogeneity. Kinetic rates for phosphorylation and complex formation were unavailable. Therefore, we assign ranges what we consider to be realistic so that the output matches with the given biological criteria. Then, we include the known qualitative features between some parameters such as protein degradation rates. For example, we consider the fact that Ime2 is an unstable protein having a higher degradation rate than Ime1. We fine-tune the parameters (Table 2) according to the following criteria: model produces transient and sequential meiosis initiation signals of its main initiators (Ime1 and Ime2) under nitrogen depletion; and the Cdk1/Cln3 and Rpd3/Sin3 levels have similar patterns to their experimental expression. In addition, we further validated the model asking biologically meaningful questions from the model based on the experimental mutant studies.

3.4 Validation of the model with experimental data

3.4.1 Time courses of key proteins

To initiate meiosis, the nitrogen depletion signal was input to the model in two ways: low constant nitrogen level, and a decreasing sigmoid function around the low nitrogen level. We present the results corresponding to the low constant nitrogen level (0.06) in Fig. 5, and similar results were observed to the other input type. Further, maximizing the nitrogen level, we checked whether the model proteins behave as expected in mitosis initiation (Fig. 8).

3.4.2 Basic mutant studies

We also checked whether our model could produce basic mutant studies related to the deletion of key genes. The deletion of Ime2 from the budding yeast cells has resulted non-transient expression of Ime1 protein. Our model also produces non-transient expression

pattern of Ime1 when the Ime2 related terms are removed from the model equation corresponding to Ime1 (Fig. 6 A). Ime1 deletion did not initiate meiosis and showed only basal Ime2 levels. When we overexpress Cln3 in very high levels (12 times higher than the usual expression in meiotic conditions), we observed a decrease in Ime1 levels relative to normal levels similar to those in the experiments (Fig. 6 B and Fig 2 of (Colomina et al., 1999)). We overexpressed Cln3 from Ime2 promoter by inserting the expression terms of Ime2 to Cln3 (Fig. 6 C), and the results matched the experiments(Gurevich et al., 2010). We also changed the Ime1 copy number according to the experiments (Gurevich et al., 2010) and observed the quadratic trend in the maximal Ime1 level to the copy number (Fig. 6 D).

4. Results

4.1 Model explains organism level results of mutant analysis in gene expression level

Since the model produced accurate results during validation, we employed the model to understand organism level results from mutant studies. The first mutant study involves the phosphorylations associated with the Ime2 protein by Cdk1/Cln3. Ime2 protein, which is activated by Cak1, possesses three potential phosphorylation sites where Cdk1 can bind and phosphorylate. When these three phosphorylation sites are blocked (Ime2-3SA), it showed a reduction in the number of budding cells compared to wild type cells, and the nitrogen depletion caused a rapid and efficient G1 arrest than the wild type (Szwarcwort-Cohen et al., 2010). Further, the mutant cells initiated meiotic S phase approximately about 4 hours pre-mutually. These results suggest that the Ime2-3SA protein was activated pre-maturely initiating the DNA replication.

To test the effects by the mutations on the Cdk1 phosphorylation sites on Ime2, we remove the term associated with Cdk1/Cln3 phosphorylations on Ime2 from our model equation of Ime1 protein. The protein levels of mutant and the normal system predicted by the model are given in the Fig. 7. The removal of phosphorylation resulted in increased levels of Ime2 protein in the early hours. The premature Ime2 protein expression predicted by the model, which is approximately 3 hours, explains the experimental observation of rapid G1 arrest and pre-mature meiotic S-phase initiation. Since MMGs and LMGs are activated by EMGs, it is conceivable that the expression patterns of MMGs and LMGs follow EMGs such as Ime2. However, it is observed from the experiments that MMGs and LMGs are not expressed during early hours similar to EMGs until a time point after which the expression followed the EMG pattern (compare EMG and MMG expressions before 6 hours in Figure 3 A of

(Gurevich et al., 2010)). Our model prediction of the post-translational (via phosphorylation) reduction of Ime2 levels at early hours would not activate the MMGs and LMGs in early hours matching with the experimental results in Figure 3A of (Gurevich et al., 2010). The experimental Ime2 protein expression by beta-gal assays provides a measure of Ime2 protein expression before post-translational modifications (marked by filled circles in Fig. 7). Accordingly, when the post-translational modification of phosphorylations is removed, the model output matches with the Ime2 expression data.

4.2 Mitosis Initiation

The model predicts that meiosis initiator (Ime1 and Ime2) levels are low and mitosis initiator (Cdk1/Cln3) levels are high in rich nitrogen levels (Fig. 8). These results are consistent with the experimental results; Ime1 is in undetectable levels, and Ime2 is absent in the nucleus during vegetative conditions (Sagee et al., 1998). According to experiments, expression of Ime2 in vegetative cultures is toxic(Guttmann-Raviv et al., 2002). The Rpd3/Sin3 complex on the promoters shows high value in our model output. This is reasonable because high amount of Rpd3/Sin3 resides on IME2 promoters to repress IME2 expression during rich nitrogen conditions.

4.3 Switch between meiosis and mitosis initiators

Nullcline analysis is frequently used in bistable system analysis (Ferrell, 2008; Tóth et al., 2007). In our ODE model, we study each pair of balance curves of all the combinations of variables throughout a range of nutritional conditions, starting from low value to a very high value. Among all the variable pairs, the nullcline analysis between meiosis and mitosis inducers shows single steady state in nitrogen starved conditions, which may correspond to the meiosis state (Fig. 9 A). The meiosis initiator (Ime2) level of this steady state is higher than the mitosis initiator (Cdk1/Cln3) level. When nutritional conditions are further increased from the lowest level, we observe three intersection points (steady states) in the same variable pair (Fig. 9 B). Further higher nutritional levels show single steady state, which may correspond to the mitosis state, where the mitosis inducer levels are higher than the meiosis inducer levels (Fig. 9 C).

We examined the global steady states in our model by equating the rate changes of all the proteins to zero and did not find any unique steady state. At the same time, by global stability analysis we could not identify any of the previously discussed (Fig. 9) intersection points between Ime2 and Cdk1/Cln3 nullclines as global, stable steady states. This is because the other two variables (Ime1 and Rpd3/Sin3) are not in steady states at any of the steady states for Ime2 and Cdk1/Cln3. This is reasonable because Ime2 and Cdk1/Cln3 are the major meiosis and mitosis initiators, and other two proteins are helping their transient expression patterns. This problem is normally addressed by reducing the equation set into a two dimensional model of interested proteins with pseudo steady state approximations and assumptions for other proteins (Tóth et al., 2007; Toth Attila, 2004). However, we cannot reduce the equations in a meaningful manner because of the nature of relations between the variables. For example, we do not have any Sin3/Rpd3 involvement in the right-hand side of equation 1 or 4.

With the intention of studying the local stability of Ime2 and Cdk1/Cln3 steady states, we study the effect of the levels of Ime1 and Rpd3/Sin3 on the steady states of Ime2 and Cdk1/Cln3. For this purpose, we consider a 5 hour time period around the Ime2 peak value where the Ime2 protein can be considered as fully expressed. During this time period, we study the effects on our interested balance curves (Ime2 and Cdk1/Cln3) by the values (mainly average value and the values at arbitrary selected time points) of Ime1 and Rpd3/Sin3. First, using the average Ime1 and Rpd3/Sin3 values during the selected 5 hour time period as the steady states of Ime1 and Rpd3/Sin3, we examine the other two proteins' nullcline behaviours. We also use arbitrary time points from the selected 5 hour time period and study how the values of Ime1 and Rpd3/Sin3 at those time points affect the Cdk1/Cln3 and Ime2 nullcline behaviour. The Ime2 balance curve does not change its entire shape, but it changes the curvature for the different Ime1 and Rpd3/Sin3 average values (Fig. 10 A). However, a steady state corresponding to meiosis is found at the intersection of nullclines for the average value pair and arbitrary time points. This intersection point has a gradual variation in its Ime2 value for changing Ime1 and Rpd3/Sin3 levels. However, the shape of the Cdk1/Cln3 balance curve does not change for the average values of Ime1 and Rpd3/Sin3, because Cdk1/Cln3 nullcline equation does not include any Ime1 and Rpd3/Sin3 variables.

We repeated the aforementioned procedure at the nitrogen level (0.083), where we found three steady states. The results (Fig. 10 C) show that there exist three intersection points regardless of the Ime1 and Rpd3/Sin3 variation mainly for the mean value of five hours and

at the time of maximum Ime2 expression. This nitrogen level is more unstable than the other two levels since it is the transition state. Further, at higher nitrogen levels (Fig. 10 B), we found one nullcline intersection point, corresponding to mitosis initiation.

Ime1 and Rpd3/Sin3 levels do not affect the number of steady states between two initiators in the system for any nitrogen condition, except the existence of slight variations in the steady state values. We conclude that the existence of the bistable switch in Ime2 or Cdk1/Cln3 is not affected by supporting protein (Ime1 and Rpd3/Sin3) variations.

4.4 Nutritional dependence of the switch between meiosis and mitosis

We use the bifurcation analysis to examine the meiosis and mitosis initiator behaviour for the whole range of nitrogen, assuming Ime1 and Sin3/Rpd3 remain at steady state levels. These steady state levels of Ime1 and Rpd3/Sin3 are assumed to be the mean values corresponding to time segment of length 2 hours which includes the maximum meiosis initiator (Ime2) level. This time segment is chosen because it is the most probable Ime2 steady state as the Ime2 level decreases or increases outside of this time interval (Fig. 5). We conducted the bifurcation analysis considering the nitrogen level as the bifurcation parameter (Fig. 11).

The switch shows that meiosis initiates only at limited nitrogen conditions matching with experiments (Kassir et al., 2003). Both Ime2 and Cdk1/Cln3 show two steady states corresponding to meiosis and mitosis separated by one unstable steady state, which are key characteristics of a bistable switch (Morgan, 2006). We observed the gap between the threshold steady states of meiosis and mitosis initiation is around (0.1=10nM), which would be sufficient for mutually exclusive initiation of these two processes.

4.5 Transition between meiosis and mitosis

The transition from mitosis to meiosis initiation is predicted to occur between 0.08 and 0.09 of the maximum nitrogen level of 1. We notice saddle node bifurcation from bistable state to meiosis state when the nitrogen level is decreased from the transition region. The saddle node bifurcation again appears at the transition to mitosis state.

This observed nutrient dependent switch is reversible since the transition period is extremely narrow. Because of this reversibility, a cell which has decided to undergo meiosis (because of nutrient stress conditions) would change its decision if the nutrient condition changes favouring mitosis initiation. In fact, the experiments have revealed that budding yeast cells can choose between meiosis or mitosis initiation according to the available nutrients until an irreversible point called 'commitment point'(Simchen, 2009). Such flexible decision making is required for the optimum usage of the nutrients for the survival of the organism.

5. Discussion

We present a theoretical model, based on well thought-through assumptions, of meiotic-mitotic switch in *Saccaromyces cerevisiae* diploid cells based on the relations between meiosis, mitosis initiators and available nutrients. The model consists of four differential equations and forty parameters. Our model predicts a nitrogen based bistable switch of major initiators (Ime2 and Cdk1/Cln3), which consists of two stable states corresponding to meiosis and mitosis initiation states. The unique features of the current study compared with previous studies are that: (1) the model incorporates the regulation of both meiosis (Ime1, Ime2) and mitosis (Cdk1/Cln3) initiators; (2) the model is investigated in a range of nutrient conditions; and (3) the model equations are non-dimentionalized so the results are easily comparable with available relative protein levels.

The predicted switch in meiosis initiator is turned on to meiosis initiation stage when the nitrogen level is starved as shown by the experiments (Fig.1 of (Kassir et al., 2003)); and, the switch in mitosis initiator is turned on at abundant nutrient levels which agrees with the experiments as well (Gallego et al., 1997). Our modelled switch explains the mutually exclusive existence of these two developmental processes by a substantial gap (unstable steady state) between the threshold levels of the two stable states. The predicted switch is reversible that once the meiosis switch is turned on by nutritional stress, it would change its decision to mitosis initiation if high levels of nutrients are provided. This is experimentally evident by the observation of the return to growth (mitosis) in meiosis decided cells if exposed to nutrients before they reach the meiotic commitment point. The similar reversible behaviour according to available nutrients is observed in mitosis decided cells until they reach the mitotic commitment point (Simchen, 2009).

The model accurately and qualitatively explains mutant studies carried out experimentally. Specifically, the model reproduces the Cdk1/Cln3 related repression on Ime1 and Ime2 (Fig. 6) which was experimentally tested by two different ways: Overexpressing Cln3 by Ime2 promoter (Gurevich et al., 2010), and overexpressing Cln3 using a tetracycline regulatory system (Colomina et al., 1999). These two ways have overexpressed Cln3 at two different concentration levels since the former experiment caused only a two hours delay in entering pre-meiotic DNA replication while the latter caused doubling the number of cells (driving cells to mitosis initiation) and arrested a high percentage of cells with 4c DNA content presumably by higher Cln3 overexpression compared to the former experiment. Our model verifies and reproduces the two experimental observations when Cln3 is overexpressed from Ime2 promoter (Fig. 6 C) and when Cln3 is overexpressed at a higher level than the former experiment (Fig. 6B).

Mutually exclusive existence of meiosis and mitosis requires a bistable switch in its initiators with a substantial gap between the two stable steady states. The requirements for a bistable switch include a feedback loop such as double negative or positive in which the two legs of the feedback loop are properly balanced. It was initially suggested that Cln3 repression on Ime1 would help to explain the incompatibility of meiosis and mitosis (Colomina et al., 1999). However, our model does not show a bistable switch between Ime1 and Cln3 by nullcline analysis, but shows a bistable switch only between Ime2 and Cln3. This is possible since the negative cross talk between Ime1 and Cln3 is uni-directional and it is experimentally revealed that meiosis is robust to decreased or increased levels of IME1 RNA(Gurevich et al., 2010).

In summary, we show meiosis and mitosis initiators create bistable switches with two alternative stable states corresponding to mitosis and meiosis states. The transition to and from each state happens via a small region where the two steady states coexist. The cell would transit from meiosis to mitosis or vice versa from saddle node bifurcation. Due to the narrow region of coexistence of two steady states, the proposed switch is reversible which helps the optimal usage of available nutrients. Once a cell decides to undergo meiosis in stress nutrients, if the nutrients are additionally provided, cell would return to growth (mitosis initiation) and vice-versa until they reach commitment point as shown in the experiments (Simchen, 2009).

The nutritional dependence of yeast cell division decision can be considered as a survival strategy of an organism. In fact, meiosis produces unique gametes which may survive hash nutritional conditions. Mitosis type cell division creates identical cell copies for the continuation of the cell generation. The reversible switch between these two processes would allow the cells to choose between these two types of cell divisions for the optimal usage of available nutrients for survival and growth of the organism.

Table A.1 The set of non-dimentionalised equations.

$$\frac{df\overline{\mathrm{Ime}l}}{dt}=\frac{\alpha_{f\mathrm{Ime}l}}{f\mathrm{Ime}l_o}+\frac{\beta_{f\mathrm{Ime}l}}{f\mathrm{Ime}l_o}\left[\left(\frac{\overline{f\mathrm{Ime}l}^{n1}}{(K_{f\mathrm{Ime}l1}/f\mathrm{Ime}l_o)^{n1}+\overline{f\mathrm{Ime}l}^{n1}}\right)\left(\frac{K_{N_2}^{n_2}}{K_{N_2}^{n_2}+(N_{2o}\overline{N_2})^{n_2}}\right)\left(\frac{K_{Rpd3S\mathrm{Ime}l}^{n_{11}}}{K_{Rpd3S\mathrm{Ime}l}^{n_{11}}+(\overline{Rpd3S}Rpd3S_o)^{n_{11}}}\right)\left(\frac{K_{Cdk1\backslash C\ln 3}^{n_9}}{K_{Cdk1\backslash C\ln 3}^{n_9}+(Cdk1\backslash C\ln 3_o\,\overline{Cdk1\backslash C\ln 3})^{n_9}}\right)\right]$$
$$-\frac{\gamma_{P\mathrm{Ime}lC\ln 3}}{f\mathrm{Ime}l_o}\left(\frac{\overline{Cdk\backslash C\ln 3}^{n_{10}}}{\overline{Cdk1\backslash C\ln 3}^{n_{10}}+(K_{P\mathrm{Ime}lCdk1\backslash C\ln 3}/Cdk1\backslash C\ln 3_o)^{n_{10}}}\right)$$
$$-d_{f\mathrm{Ime}l}(\overline{f\mathrm{Ime}2})(\overline{f\mathrm{Ime}l})(f\mathrm{Ime}2_o) \quad \text{(A1)}$$

$$\frac{d\overline{f\mathrm{Ime}2}}{dt}=\frac{\alpha_{f\mathrm{Ime}2}}{f\mathrm{Ime}2_o}+\frac{\beta_{f\mathrm{Ime}2}}{f\mathrm{Ime}2_o}\left[\left(\frac{\overline{f\mathrm{Ime}2}^{n_3}}{\left(\frac{K_{f\mathrm{Ime}22}}{f\mathrm{Ime}2_o}\right)^{n_3}+\overline{f\mathrm{Ime}2}^{n_3}}\right)\left(\frac{\overline{f\mathrm{Ime}l}^{n_4}}{\left(\frac{K_{f\mathrm{Ime}12}}{f\mathrm{Ime}l_o}\right)^{n_4}+\overline{f\mathrm{Ime}l}^{n_4}}\right)\left(\frac{K_{Rpd3\backslash Sin3}^{n_5}}{K_{Rpd3\backslash Sin3}^{n_5}+(Rpd3\backslash Sin3_o\,\overline{Rpd3\backslash Sin3})^{n_5}}\right)\right]$$
$$-\frac{\gamma_{P\mathrm{Ime}2}}{f\mathrm{Ime}2_o}\left(\frac{\overline{Cdk1\backslash C\ln 3}^{n_6}}{\overline{Cdk1\backslash C\ln 3}^{n_6}+\left(\frac{K_p}{Cdk1\backslash C\ln 3_o}\right)^{n_6}}\right)$$
$$-d_{f\mathrm{Ime}2}\left(\overline{f\mathrm{Ime}2}\right) \quad \text{(A2)}$$

$$\frac{d\overline{Cdk1\backslash C\ln 3}}{dt} = \frac{\alpha_{C\ln 3}}{Cdk1\backslash C\ln 3_o} + \frac{\beta_{Cdk1\backslash C\ln 3}}{Cdk1\backslash C\ln 3_o}\left(\frac{\overline{N}_2^{n_7}}{\left(\frac{K_{N_{2C\ln 3}}}{N_{2o}}\right)^{n_7} + \overline{N}_2^{n_7}}\right) - \frac{\gamma_{PCdk1C\ln 3}}{Cdk1\backslash C\ln 3_o}\left(\frac{\overline{f\,\mathrm{Im}e2}^{n_8}}{\left(\frac{K_{P\mathrm{Im}e2Cdk1}}{f\,\mathrm{Im}e2_o}\right)^{n_8} + \overline{f\,\mathrm{Im}e2}^{n8}}\right) - d_{C\ln 3}(\overline{Cdk1\backslash C\ln 3}) \quad \text{(A3)}$$

$$\frac{d\overline{Rpd3\backslash Sin3}}{dt} = \frac{\alpha_{Rpd3Sin3}}{Rpd3\backslash Sin3_o} - d_{Rpd3Sin3}\frac{\overline{fIme1}fIme1_o}{Rpd3\backslash Sin3_0}\overline{Rim15}Rim15_o \quad \text{(A4)}$$

where

$$Rpd3S = \left(n_{12} - \left(n_{12}\left(1 - exp\left(t-6\right)\right)\right)\right)$$

$$Rim15 = \frac{1}{N_2\, N_{2o}}\left(\frac{n_{13}}{n_{15} + \exp(1.6t)} + n_{14}\right)$$

Appendix A

Table A.1: The set of non-dimentionalised equations.

List of Figures

Fig. 1. Nutritional dependence of mitosis and meiosis initiation of budding yeast diploid cells. Nutritional stress activates IME1 expression and inhibits the cell cycle entry by down-regulating Cdk1/Cln3. Ime2 expression, stimulated by Ime1, then activates the expression of Middle meiosis specific genes (MMGs) including the gene, NDT80. Afterwards, Ndt80 and

Ime2 activate the transcription of MMGs. Transcription of further downstream meiotic genes depends indirectly on Ime1, Ime2 and Ndt80. Entry into mitosis is activated by the rising Cdk1/Cln3 activity generated by good nutritional conditions, which inhibit meiosis initiation at the same time. Cln3 has key roles in timely activation of the transcription factors, SBF (Swi4-Swi6) and MBF (Mbp1-Swi6) dependent promoters in late G1; afterwards, the flows of regulatory signals activate the appropriate Cyclin dependent kinases (Cdks) and regulatory signals leading to ordered progression of the cell cycle.

Fig. 2. The schematic diagram of the model showing the regulatory mechanisms of meiosis and mitosis initiation**.** Nitrogen depletion inhibits mitosis initiation by repressing Cln3 and helps meiosis initiation by activating Ime1 expression and relieving Rpd3/Sin3 repression from EMGs via Rim15. Rising Ime1 levels activate IME2 transcription and relieve Rpd3/Sin3 repression. Ime2 activates the further downstream meiotic genes and phosphorylates Ime1 tagging it for degradation. Ime2 inhibits Cdk1/Cln3 functionality and prevents mitosis. Good nitrogen conditions activate the Cln3 expression for mitosis initiation. Cdk1s activated by Cln3 initiate the mitosis cell cycle. Meiosis initiation is inhibited during mitosis by the Ime2 deactivation by Cdk1 phosphorylation and the transcriptional repression of Ime1 by Cln3; at the same time, the phosphorylated Ime1 by Cln3 is transported out of the nucleus which is instead modelled as degradation inside the nucleus.

Fig. 3. The modelled Rpd3S temporal variation according to the Equation 1.1.

Fig. 4. The modelled active Rim15 temporal variation according to equation 4.1. (A) Upon transferring to meiotic conditions, Rim15 is active but is not transcribed, therefore the available Rim15 protein amount degrades. (B) At good nutrients, Rim15 protein is inactivated by phosphorylation, therefore Rim15 levels are negligible.

Fig. 5. The modelled meiosis initiation related protein variation in the sporulation medium (SPM). The circles and their error bars represent the scaled data from the Ime1 protein expression patterns measured in Beta-Galactose (β gal) units from (Shefer-Vaida et al., 1995). Filled circles represent the scaled data from Fig. 7 B of (Gallego et al., 1997). Squares represent the scaled data from Fig. 2D of (Pnueli et al., 2004). Initial conditions for the model were within the normal range under which meiosis initiation occurs: 0.1 for Ime1 and 0.6 for the Rpd3/Sin3 concentration, 0.06 for nitrogen concentration, 0.1 for Cln3 and 0 for the other proteins (Gallego et al., 1997; Rubinstein et al., 2007).

Fig. 6. Predicted mutant analysis results. (A) Deletion of Ime2 results an increase in the Ime1 protein levels. The filled circles represent the scaled data from the Ime1 protein expression from Fig. 1 of (Shefer-Vaida et al., 1995). (B) When Cln3 is overexpressed twelve times more than the normal meiotic Cln3 expression, the model shows low Ime1 levels compared with normal expression of Ime1. (C) Ime1 expression when Cln3 is overexpressed from IME2 promoter. (D) When Ime1 copy number is changed, the maximal level of Ime1 and IME1 copy number approximately fit to a quadratic trend. The equation of the trend line is given inside the figure (Initial conditions are similar to the experiments (Gurevich et al., 2010)).

Fig. 7. The post-translational modification removal in Ime2. The model output when the post-translational phosphorylations are removed (continuous line) shows higher Ime2 protein levels than the wild type (dashed line) in early hours. The experimental data of Ime2 expression measured by yellow fluorescent protein (YFP) levels (Filled circles representing the scaled data from several trajectories of Ime2 protein in Figure 2 A of (Nachman et al., 2007)) match with the predicted mutant behaviour since the post-translational modifications are removed during mutant analysis. Initial conditions for the model were within the normal range under which meiosis initiation occurs: 0.1 for Ime1 and 0.6 for the Rpd3/Sin3 concentration, 0.06 for nitrogen concentration, 0.1 for Cln3 and 0 for the other proteins (Gallego et al., 1997; Rubinstein et al., 2007).

Fig 8. The behaviour of proteins in high nitrogen (at the level of 1). The meiosis initiator levels are low, and mitosis initiator levels are high. Stars represent the scaled Cln3 expression data from Fig. 7 B of (Gallego et al., 1997). Initial conditions other than nitrogen were set as stated in Fig. 7.

Fig. 9. Nullcline analysis between meiosis (Ime2) and mitosis (Cdk1/Cln3) inducers. (A), (B) and (C) show the balance curves at the meiosis initiation conditions (at the nitrogen level of 0.06), at the transition from meiosis to mitosis (at the nitrogen level of 0.083) and at mitosis initiation conditions (at the nitrogen level of 0.98), respectively. The filled circles indicates the intersection points.

Fig. 10. The effect of different steady state levels of Ime1 and Rpd3/Sin3 on nullcline intersection points. The number of intersection points observed for different nutritional conditions is unchanged regardless of the average steady state level of other proteins. (A) Nullcline plot for low nitrogen conditions (0.06). (B) One intersection point is found at higher

nitrogen conditions (0.98). (C) Nullcline plot for nitrogen condition (0.083) with three intersection points. Intersection points are indicated with coloured circles.

Fig. 11. Bifurcation diagram considering nitrogen relative level as the bifurcation parameter. Stable steady states are bold, and the unstable steady states are drawn with dashed lines. (A) The switch of Ime2. (B) The nutritional dependence of Cdk1/Cln3. (C) and (D) show the enlarged switch in Ime2 and Cdk1/Cln3, respectively. Shaded area shows the gap between the states corresponding to meiosis and mitosis.

List of Tables

Table 1. Initial parameter ranges used for parameter estimation (Biological significance of the parameters are given in Table 2).

Table 2. Parameters, their biological significance and values.

References

Alon, U., 2007. An introduction to systems biology: design principles of biological circuits. CRC press.

Angeli, D., Ferrell, J. E., Sontag, E. D., 2004. Detection of multistability, bifurcations, and hysteresis in a large class of biological positive-feedback systems. Proceedings of the National Academy of Sciences of the United States of America 101, 1822, doi:10.1073/pnas.0308265100

Barik, D., Baumann, W. T., Paul, M. R., Novak, B., Tyson, J. J., 2010. A model of yeast cell-cycle regulation based on multisite phosphorylation. Molecular Systems Biology 6.

Burgess, S. M., Ajimura, M., Kleckner, N., 1999. GCN5-dependent histone H3 acetylation and RPD3-dependent histone H4 deacetylation have distinct, opposing effects on IME2 transcription, during meiosis and during vegetative growth, in budding yeast. Proceedings of the National Academy of Sciences 96, 6835-6840.

Chen, K. C., Csikasz-Nagy, A., Gyorffy, B., Val, J., Novak, B., Tyson, J. J., 2000. Kinetic analysis of a molecular model of the budding yeast cell cycle. Molecular Biology of the Cell 11, 369.

Chen, K. C., Calzone, L., Csikasz-Nagy, A., Cross, F. R., Novak, B., Tyson, J. J., 2004. Integrative analysis of cell cycle control in budding yeast. Molecular Biology of the Cell 15, 3841, doi:10.1091/mbc.E03-11-0794

Colomina, N., Garí, E., Gallego, C., Herrero, E., Aldea, M., 1999. G1 cyclins block the Ime1 pathway to make mitosis and meiosis incompatible in budding yeast. The EMBO Journal 18, 320-329, doi:10.1093/emboj/18.2.320.

de Bruin, R. A. M., McDonald, W. H., Kalashnikova, T. I., Yates, J., Wittenberg, C., 2004. Cln3 Activates G1-Specific Transcription via Phosphorylation of the SBF Bound Repressor Whi5. Cell 117, 887-898, doi:10.1016/j.cell.2004.05.025.

De Vries, G., 2006. A course in mathematical biology: quantitative modeling with mathematical and computational methods. Society for Industrial Mathematics.

Dushek, O., vanáderáMerwe, P. A., Shahrezaei, V., 2011. Ultrasensitivity in Multisite Phosphorylation of Membrane-Anchored Proteins. Biophysical Journal 100, 1189-1197, doi:10.1016/j.bpj.2011.01.060.

Ferrell, J. E., 2008. Feedback regulation of opposing enzymes generates robust, all-or-none bistable responses. Current Biology 18, R244-R245, doi:10.1016/j.cub.2008.02.035.

Forsburg, S. L., Nurse, P., 1991. Cell cycle regulation in the yeasts Saccharomyces cerevisiae and Schizosaccharomyces pombe. Annual review of cell biology 7, 227-256, doi:10.1146/annurev.cb.07.110191.001303.

Gallego, C., Gari, E., Colomina, N., Herrero, E., Aldea, M., 1997. The Cln3 cyclin is down-regulated by translational repression and degradation during the G1 arrest caused by nitrogen deprivation in budding yeast. EMBO J 16, 7196-7206, doi:10.1093/emboj/16.23.7196.

Gupta, P. K., 2009. Cell and Molecular Biology. Global Media, Meerut, IND.

Gurevich, V., Kassir, Y., Idnurm, A., 2010. A switch from a gradient to a threshold mode in the regulation of a transcriptional cascade promotes robust execution of meiosis in budding yeast. PloS one 5, e11005, doi:10.1371/journal.pone.0011005

Guttmann-Raviv, N., Martin, S., Kassir, Y., 2002. Ime2, a meiosis-specific kinase in yeast, is required for destabilization of its transcriptional activator, Ime1. Molecular and cellular biology 22, 2047, doi:10.1128/MCB.22.7.2047-2056.2002.

Harvey Lodish, A. B., Paul Matsudaira, S. Lawrence Zipursky, David Baltimore, James Darnell, 1995. Molecular Cell Biology. Scientific American Books.

Holt, L. J., Hutti, J. E., Cantley, L. C., Morgan, D. O., 2007. Evolution of Ime2 phosphorylation sites on Cdk1 substrates provides a mechanism to limit the effects of the phosphatase Cdc14 in meiosis. Molecular cell 25, 689-702, doi:10.1016/j.molcel.2007.02.012.

Hong, C., Lee, M., Kim, D., Kim, D., Cho, K.-H., Shin, I., 2012. A checkpoints capturing timing-robust Boolean model of the budding yeast cell cycle regulatory network. BMC Systems Biology 6, 129.

Kaizu, K., Ghosh, S., Matsuoka, Y., Moriya, H., Shimizu-Yoshida, Y., Kitano, H., 2010. A comprehensive molecular interaction map of the budding yeast cell cycle. Molecular Systems Biology 6.

Kassir, Y., Adir, N., Boger-Nadjar, E., Raviv, N. G., Rubin-Bejerano, I., Sagee, S., Shenhar, G., 2003. Transcriptional regulation of meiosis in budding yeast. International review of cytology 224, 111-171, doi:10.1016/S0074-7696(05)24004-4.

Kominami, K., Sakata, Y., Sakai, M., Yamashita, I., 1993. Protein kinase activity associated with the IME2 gene product, a meiotic inducer in the yeast Saccharomyces cerevisiae. Bioscience, biotechnology, and biochemistry 57, 1731, doi:10.1271/bbb.57.1731.

Lu, P., Vogel, C., Wang, R., Yao, X., Marcotte, E. M., 2006. Absolute protein expression profiling estimates the relative contributions of transcriptional and translational regulation. Nature biotechnology 25, 117-124, doi:10.1038/nbt1270.

Mehta, P., Mukhopadhyay, R., Wingreen, N. S., 2008. Exponential sensitivity of noise-driven switching in genetic networks. Physical Biology 5, 026005, doi:10.1088/1478-3975/5/2/026005.

Miller, M. E., Cross, F. R., 2001. Cyclin specificity: how many wheels do you need on a unicycle? Journal of Cell Science 114, 1811-1820.

Morgan, D., 2006. The Cell Cycle: Principles of Control (Primers in Biology Series).

Nachman, I., Regev, A., Ramanathan, S., 2007. Dissecting Timing Variability in Yeast Meiosis. Cell 131, 544-556, doi:10.1016/j.cell.2007.09.044.

Novak, B., Tyson, J. J., 2004. A model for restriction point control of the mammalian cell cycle. Journal of theoretical biology 230, 563-579, doi:10.1016/j.jtbi.2004.04.039.

Parviz, F., Heideman, W., 1998. Growth-Independent Regulation of CLN3mRNA Levels by Nutrients in Saccharomyces cerevisiae. Journal of bacteriology 180, 225-230.

Piekarska, I., Rytka, J., Rempola, B., 2010. Regulation of sporulation in the yeast Saccharomyces cerevisiae. Acta biochimica Polonica 57, 241-50.

Pnueli, L., Edry, I., Cohen, M., Kassir, Y., 2004. Glucose and nitrogen regulate the switch from histone deacetylation to acetylation for expression of early meiosis-specific genes in budding yeast. Molecular and cellular biology 24, 5197, doi:10.1128/MCB.24.12.5197-5208.2004

Pramila, T., Miles, S., GuhaThakurta, D., Jemiolo, D., Breeden, L. L., 2002. Conserved homeodomain proteins interact with MADS box protein Mcm1 to restrict ECB-dependent transcription to

the M/G1 phase of the cell cycle. Genes & development 16, 3034-3045, doi:10.1101/gad.1034302

Rosenfeld, N., Young, J. W., Alon, U., Swain, P. S., Elowitz, M. B., 2005. Gene regulation at the single-cell level. Science 307, 1962, doi:10.1126/science.1106914.

Rubinstein, A., Gurevich, V., Kasulin-Boneh, Z., Pnueli, L., Kassir, Y., Pinter, R. Y., 2007. Faithful modeling of transient expression and its application to elucidating negative feedback regulation. Proceedings of the National Academy of Sciences 104, 6241, doi:10.1073/pnas.0611168104

Sagee, S., Sherman, A., Shenhar, G., Robzyk, K., Ben-Doy, N., Simchen, G., Kassir, Y., 1998. Multiple and distinct activation and repression sequences mediate the regulated transcription of IME1, a transcriptional activator of meiosis-specific genes in Saccharomyces cerevisiae. Molecular and cellular biology 18, 1985.

Schaechter, M., 2011. Eukaryotic Microbes. Academic Press.

Schindler, K., Benjamin, K. R., Martin, A., Boglioli, A., Herskowitz, I., Winter, E., 2003. The Cdk-activating kinase Cak1p promotes meiotic S phase through Ime2p. Molecular and cellular biology 23, 8718-8728, doi:10.1128/MCB.23.23.8718-8728.2003

Shefer-Vaida, M., Sherman, A., Ashkenazi, T., Robzyk, K., Kassir, Y., 1995. Positive and negative feedback loops affect the transcription of IME1, a positive regulator of meiosis in Saccharomyces cerevisiae. Developmental genetics 16, 219-228, doi:10.1002/dvg.1020160302.

Shenhar, G., Kassir, Y., 2001. A positive regulator of mitosis, Sok2, functions as a negative regulator of meiosis in Saccharomyces cerevisiae. Molecular and cellular biology 21, 1603, doi:10.1128/MCB.21.5.1603-1612.2001.

Simchen, G., 2009. Commitment to meiosis: what determines the mode of division in budding yeast? Bioessays 31, 169-177, doi:10.1002/bies.200800124.

Süel, G. M., Garcia-Ojalvo, J., Liberman, L. M., Elowitz, M. B., 2006. An excitable gene regulatory circuit induces transient cellular differentiation. Nature 440, 545-550, doi:10.1038/nature04588.

Szwarcwort-Cohen, M., Kasulin-Boneh, Z., Sagee, S., Kassir, Y., 2009. Human Cdk2 is a functional homolog of budding yeast Ime2, the meiosis-specific Cdk-like kinase. Cell Cycle 8, 647-654.

Szwarcwort-Cohen, M., Gurevich, V., Sagee, S., Kassir, Y., 2010. Ectopic expression of human Cdk2 and its yeast homolog, Ime2, is deleterious to Saccharomyces cerevisiae. Cell Cycle 9, 4711-4719, doi:10.4161/cc.9.23.14088.

Tóth, A., Queralt, E., Uhlmann, F., Novák, B., 2007. Mitotic exit in two dimensions. Journal of theoretical biology 248, 560-573, doi:10.1016/j.jtbi.2007.06.014

Toth Attila, N. B., Csikasz-Nagy Attila, 2004. Modelling the regulation of the treansition between mitosis and meiosis of fission yeast Department of Applied Biotechnology and Food Science, Vol. PhD. Budapest University of Technology and Economics.

Tyson, J. J., Novak, B., 2008. Temporal organization of the cell cycle. Current Biology 18, R759-R768.

Verdugo, A., Vinod, P. K., Tyson, J. J., Novak, B., Molecular mechanisms creating bistable switches at cell cycle.

Vinod, P. K., Freire, P., Rattani, A., Ciliberto, A., Uhlmann, F., Novak, B., 2011. Computational modelling of mitotic exit in budding yeast: the role of separase and Cdc14 endocycles. Journal of the Royal Society Interface 8, 1128-1141, doi:10.1098/rsif.2010.0649

Zi, Z., Liebermeister, W., Klipp, E., 2010. A quantitative study of the Hog1 MAPK response to fluctuating osmotic stress in Saccharomyces cerevisiae. PloS one 5, e9522, doi:10.1371/journal.pone.0009522.

Table 1

Parameter description	Range (in nM and hours)	Source and description
Basal Transcription rate(TR): $\alpha_{fIme1}, \propto_{fIme2}, \propto_{Cln3}$	[2.8e-3 - 7]	Median TR is 7mRNA/hour in yeast genes and minimum TR is beyond 27mRNA/h (Pelechano et al., 2010). Basal TR reference value; 7mRNA/h = 0.14nM/h (47.1 molecules in 1nM). Calculating upper and lower limits using 0.14 as reference and allowing 50 times to vary around reference value, range becomes [2.8e-3 - 7].
Maximal transcription rate: $\beta_{fIme1}, \beta_{fIme2}, \beta_{Cln3}$	[0.012 - 218.34]	90% of yeast genes have TRs between 2-30mRNA/h. Highest transcribed genes have TR of 206 mRNA/h (Pelechano et al., 2010). Reference value for the TR minimum: 30 and maximum:206 mRNA/h. Calculating upper and lower limits using (30 - 206) mRNA/h as reference range and allowing 50 times to vary around reference values, range becomes [0.012 - 218].
Transcriptional factor(TF) disassociation rate from DNA: $K_{fIme11}, K_{N_2}, K_{fIme22}, K_{fIme12}, K_{Rpd3\backslash Sin3}, K_{Cdk1\backslash Cln3}$, $K_{Rpd3SIme1}$	[0.592 - 138.6]	As more specific data was unavailable, we used the research carried out by J.C.Dorsman et al. (Dorsman et al., 1990) who determined the disassociation half-time of yeast general TF : GFI. They determined disassociation rates for several DFI-DNA complexes and found that it varied over 70- fold. Range from table III : [0.3 - 70]min directly converting to rate [0.592-138.6]/h
Hill coefficient s: $n_1, n_2, n_3, n_4, n_5, n_6, n_7, n_{8,} n_9, n_{10}, n_{11}$	[0 - 2.8]	According to experiments of (Hao et al., 2008), Hill coefficient for activation of MAP kinases, Kss1 and Fus3 are 1.3 and 2.2 respectively. As other specific data is unavailable, considered the biologically realistic range of [0 - 2.8]
Protein degradation rate: d_{fIme1}, d_{fIme2}	[9.16e-3 - 24.15]	Archana Belle et al. (Belle et al., 2006) measured the half-life of 3751 proteins and found that half life is log normal distributed with a mean and median of 43min and Fig 1C shows maximum half-life is beyond 181mins. Therefore the degradation rate/h range was calculated directly by ln(2)/half-life is [9.16e-3 - 24.15].
Protein complex degradation rate: $d_{Rpd3Sin3,} d_{Cdk1Cln3}$	[9.16e-3 - 24.15]	

	Biological Significance	Value	Unit
α_{fIme1}	Basal Transcription rate of Ime1	0.0004	nMh^{-1}
α_{fIme2}	Basal Transcription rate of Ime2	1.9	nMh^{-1}
α_{Cln3}	Basal Transcription rate of Cln3	6.74	nMh^{-1}
$\alpha_{Rpd3Sin3}$	Complex formation rate of Rpd3/Sin3	1.2859	nMh^{-1}
β_{fIme1}	Maximal transcription rate of Ime1	17	nMh^{-1}
β_{fIme2}	Maximal transcription rate of Ime2	40.92	nMh^{-1}
$\beta_{Cdk1\backslash Cln3}$	Maximal transcription rate of Cdk1/Cln3	106.612	nMh^{-1}
K_{fIme11}	Disassociation constant of Ime1 binding to its own promoter	10	nM
K_{N_2}	Disassociation constant of Nitrogen binding to IME1 promoter	2.55	nM
d_{fIme1}	Degradation rate of Ime1 protein	0.028	$nM^{-1}h^{-1}$
n_1	Hill coefficient of Ime1 auto regulation	2.8	----
n_2	Hill coefficient of Nitrogen repression on IME1 promoter	2.8	----
K_{fIme22}	Disassociation constant of Ime2 binding to its own promoter	40.8	nM
K_{fIme12}	Disassociation constant of Ime1 binding to IME2 promoter	4.65	nM
$K_{Rpd3\backslash Sin3}$	Disassociation constant of Sin3/Rpd3 binding to IME2 promoter	33.0	nM
$K_{Cdk1\backslash Cln3}$	Disassociation constant of Cdk1/Cln3 binding to IME1 promoter	70.325	nM
$K_{Rpd3SIme1}$	Disassociation constant of Rpd3S binding to IME1 promoter	105.3	nM
γ_{PIme2}	Maximal Phosphorylation rate of Ime2 by Cdk1/Cln3	20.76	nMh^{-1}
K_p	Dephosphorylation constant of Cdk1/Cln3 from Ime2	100.99	nM
n_3	Hill coefficient of Ime2 auto regulation	2.06	----
n_4	Hill coefficient of Ime1 activation on IME2 promoter	0.5679	----
n_5	Hill coefficient of Rpd3/Sin3 repression on IME2 promoter	2.8	----

n_6	Hill coefficient of phosphorylation of Ime2 by Cdk1/Cln3	2.803	----
d_{fIme2}	Degradation rate of Ime2 protein	0.149	h^{-1}
K_{N_2Cln3}	Disassociation constant of Nitrogen binding to Cln3 promoter	19.4	nM
n_7	Hill coefficient of Nitrogen activation on Cln3 promoter	2.85	----
$\gamma_{PCdk1Cln3}$	Maximal Phosphorylation rate of Cdk1/Cln3 by Ime2	50.1	nMh^{-1}
$\gamma_{PIme1Cln3}$	Maximal Phosphorylation rate of Ime1 by Cdk1/Cln3	1.1384	nMh^{-1}
$K_{PIme2Cdk1}$	Dephosphorylation constant of Ime2 from Cdk1/Cln3	100.987	nM
$K_{PIme1Cdk1\backslash Cln3}$	Dephosphorylation constant of Ime1 by Cdk1/Cln3	125.987	nM
n_8	Hill coefficient of phosphorylation of Cdk1/Cln3 by Ime2	2.8	----
n_9	Hill coefficient of Cdk1/Cln3 repression on IME2 promoter	2.8	----
n_{10}	Hill coefficient of phosphorylation of Ime1 by Cdk1/Cln3	2	----
n_{11}	Hill coefficient of Rpd3S repression on IME1 promoter	2.8	----
n_{12}	Constant related with Rpd3S temporal variation	0.8	----
n_{13}	Constant related with Rim15 temporal variation	37	----
n_{14}	Constant related with Rim15 temporal variation	0.06	----
n_{15}	Constant related with Rim15 temporal variation	0.01	----
d_{Cln3}	Degradation rate of Cdk1/Cln3 protein complex	0.2999	h^{-1}
$d_{Rpd3Sin3}$	Degradation rate of Rpd3/Sin3 protein complex	0.05348	nMh^{-1}
$fIme1_o$	Maximum Concentration of Ime1 protein	100	nM
$fIme2_o$	Maximum Concentration of Ime2 protein	100	nM
N_{2o}	Maximum Concentration of Nitrogen	6	nM
$Sin3 / Rpd3_o$	Maximum Concentration of Sin3/Rpd3 complex	100	nM

$Cdk1/Cln3_o$	Maximum Concentration of Cdk1/Cln3 complex	100	nM
$Rpd3S_o$	Maximum Concentration of Rpd3S protein	100	nM
$Rim15_o$	Maximum Concentration of Rim15 protein	100	nM

Table 2

Belle, A., Tanay, A., Bitincka, L., Shamir, R., O'Shea, E. K., 2006. Quantification of protein half-lives in the budding yeast proteome. Proceedings of the National Academy of Sciences 103, 13004-13009.

Dorsman, J. C., Van Heeswijk, W. C., Grivell, L. A., 1990. Yeast general transcription factor GFI: sequence requirements for binding to DNA and evolutionary conservation. Nucleic acids research 18, 2769-2776.

Hao, N., Nayak, S., Behar, M., Shanks, R. H., Nagiec, M. J., Errede, B., Hasty, J., Elston, T. C., Dohlman, H. G., 2008. Regulation of cell signaling dynamics by the protein kinase-scaffold Ste5. Molecular cell 30, 649.

Pelechano, V., Chávez, S., Pérez-Ortín, J. E., 2010. A complete set of nascent transcription rates for yeast genes. PloS one 5, e15442.

Highlights

- A mathematical model explains bistable meiotic-mitotic initiation switch in budding yeast.
- The proposed switch explains the reversible nutrient dependent, early stage switching between meiosis and mitosis.
- The switch explains the mutually exclusive existence of meiosis and mitosis pathway initiation.

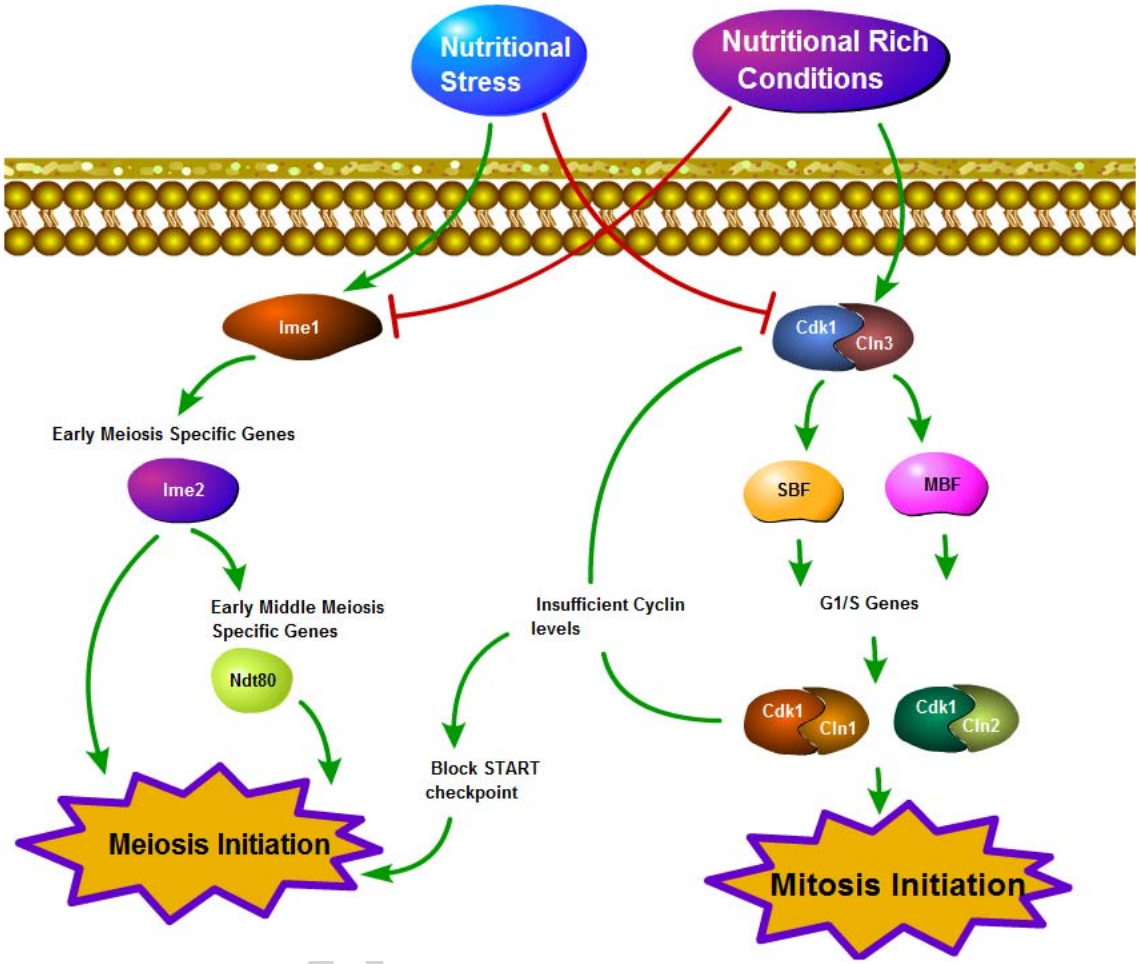

Figure 1

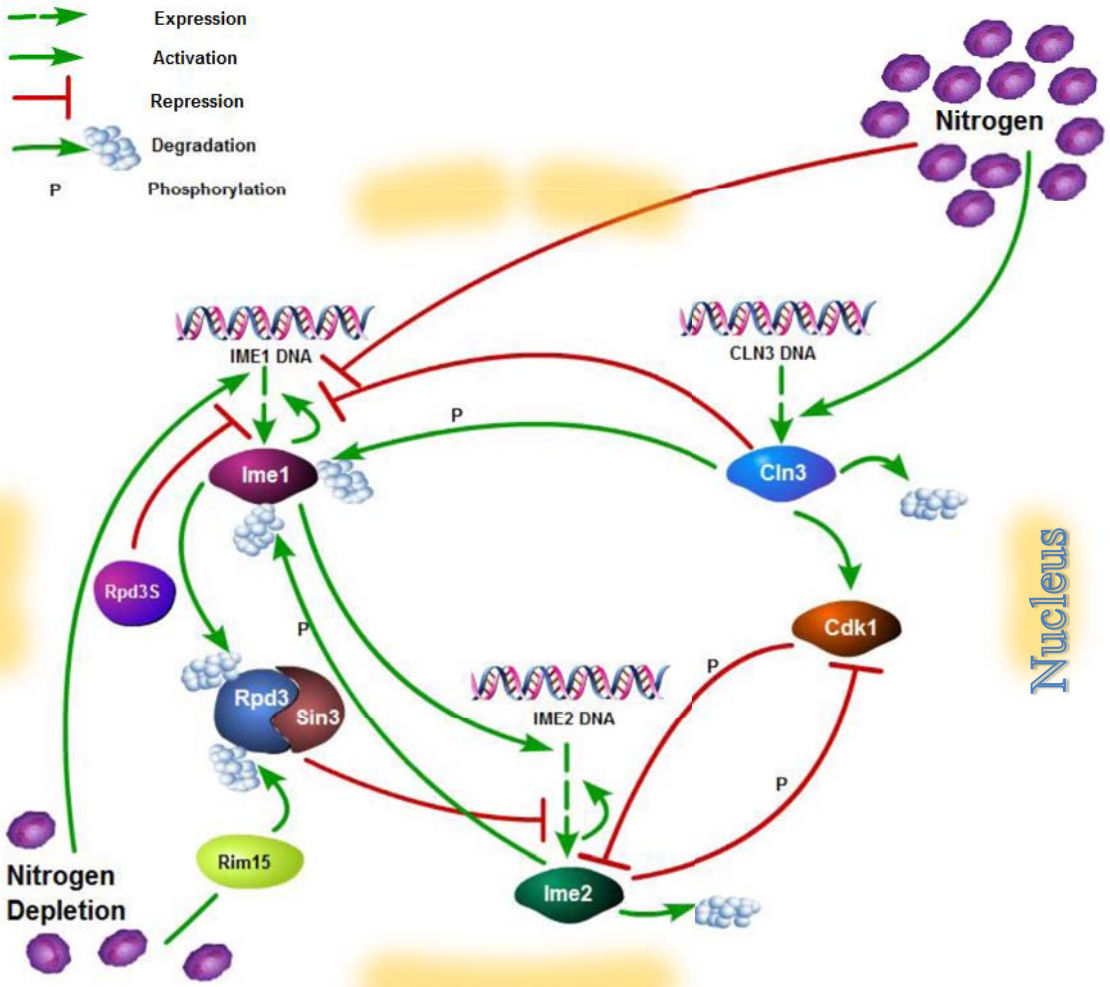

Figure 2

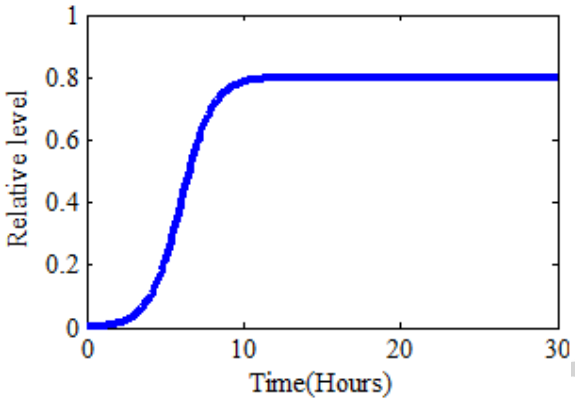

Figure 3

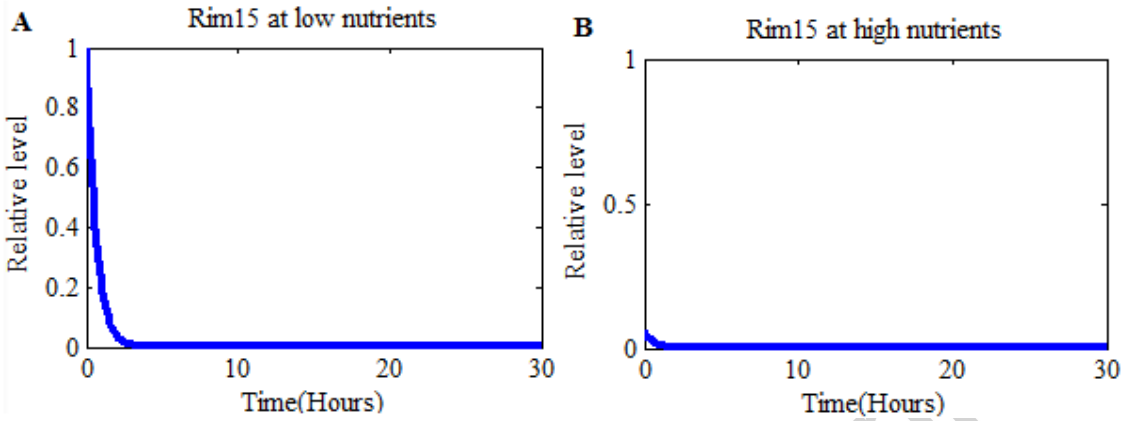

Figure 4

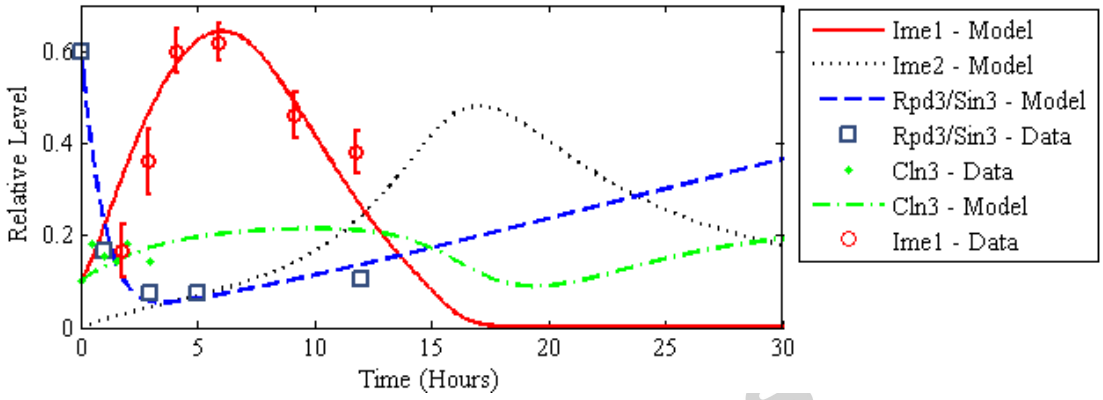

Figure 5

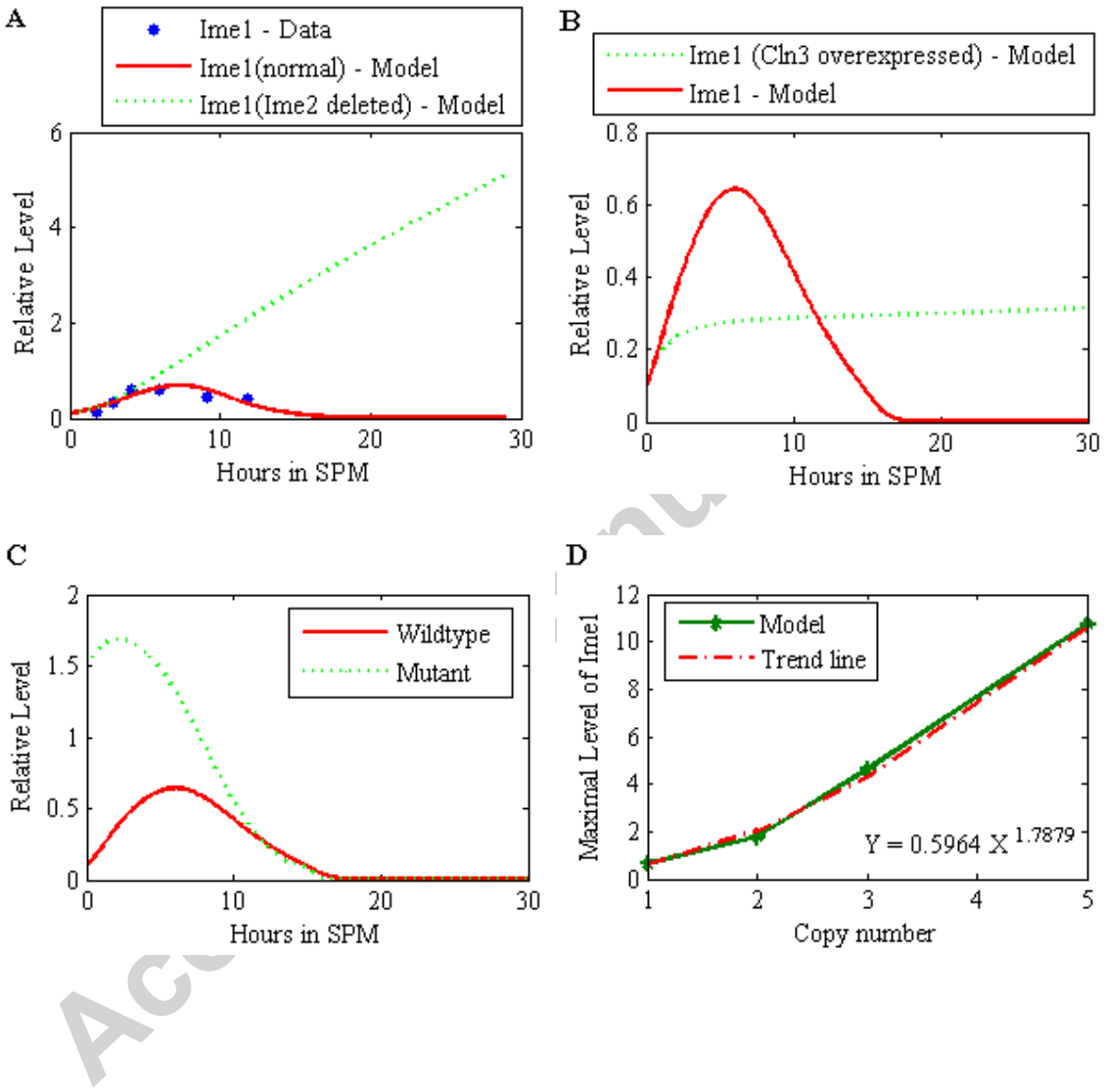

Figure 6

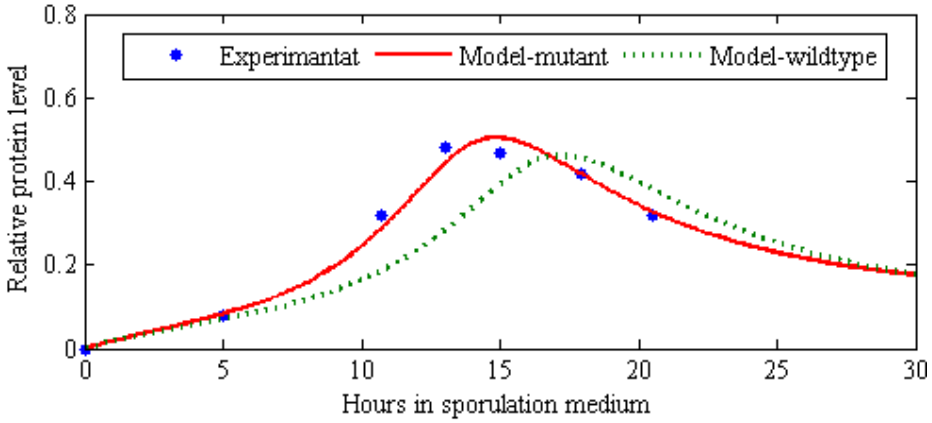

Figure 7

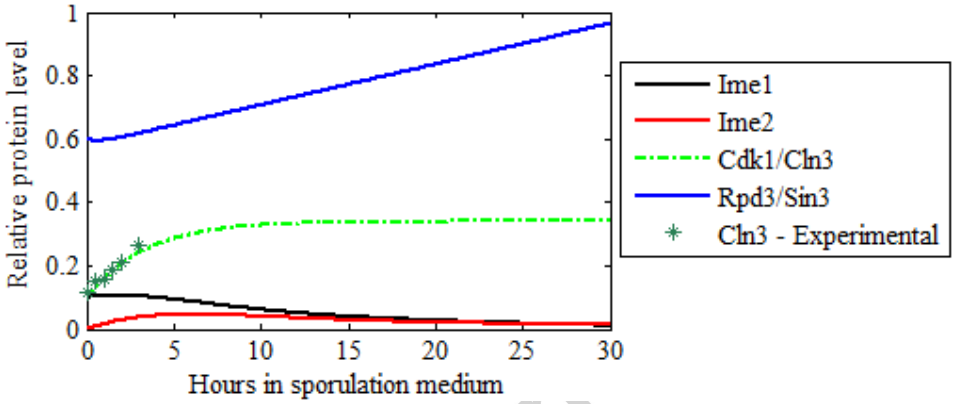

Figure 8

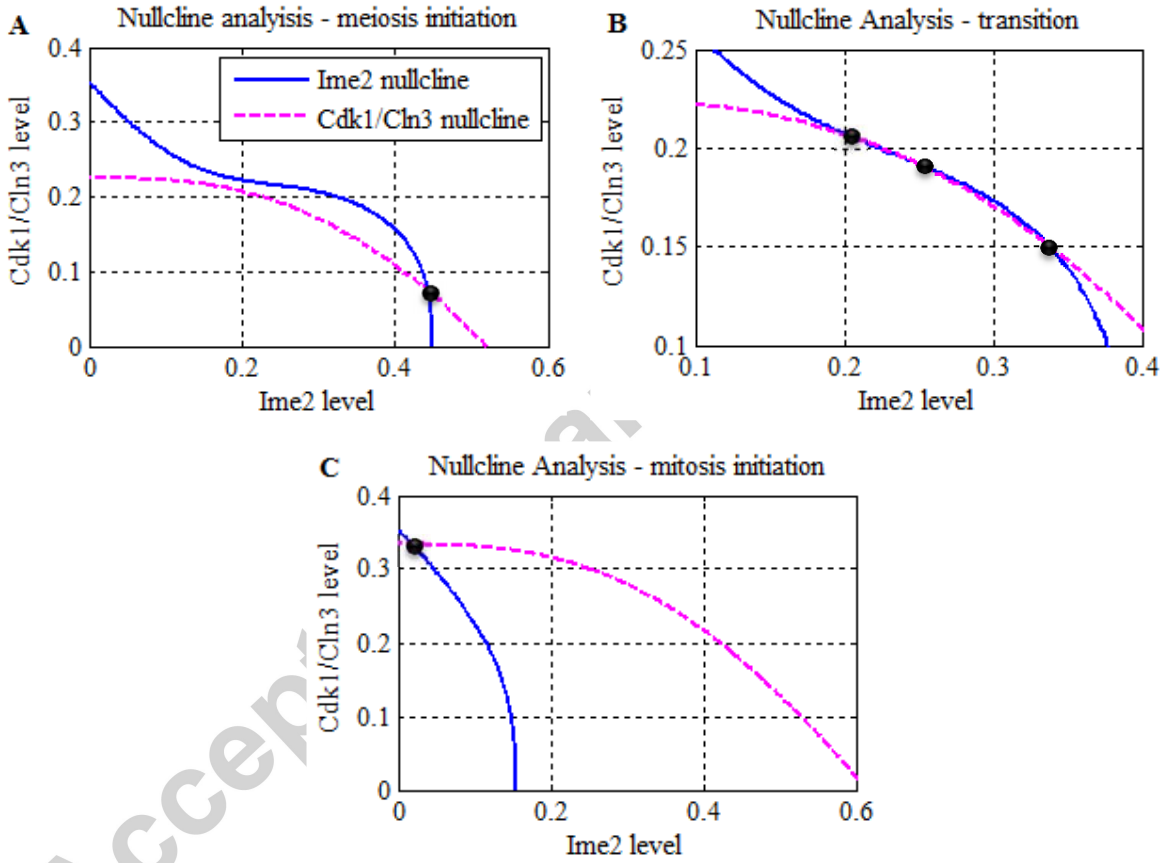

Figure 9

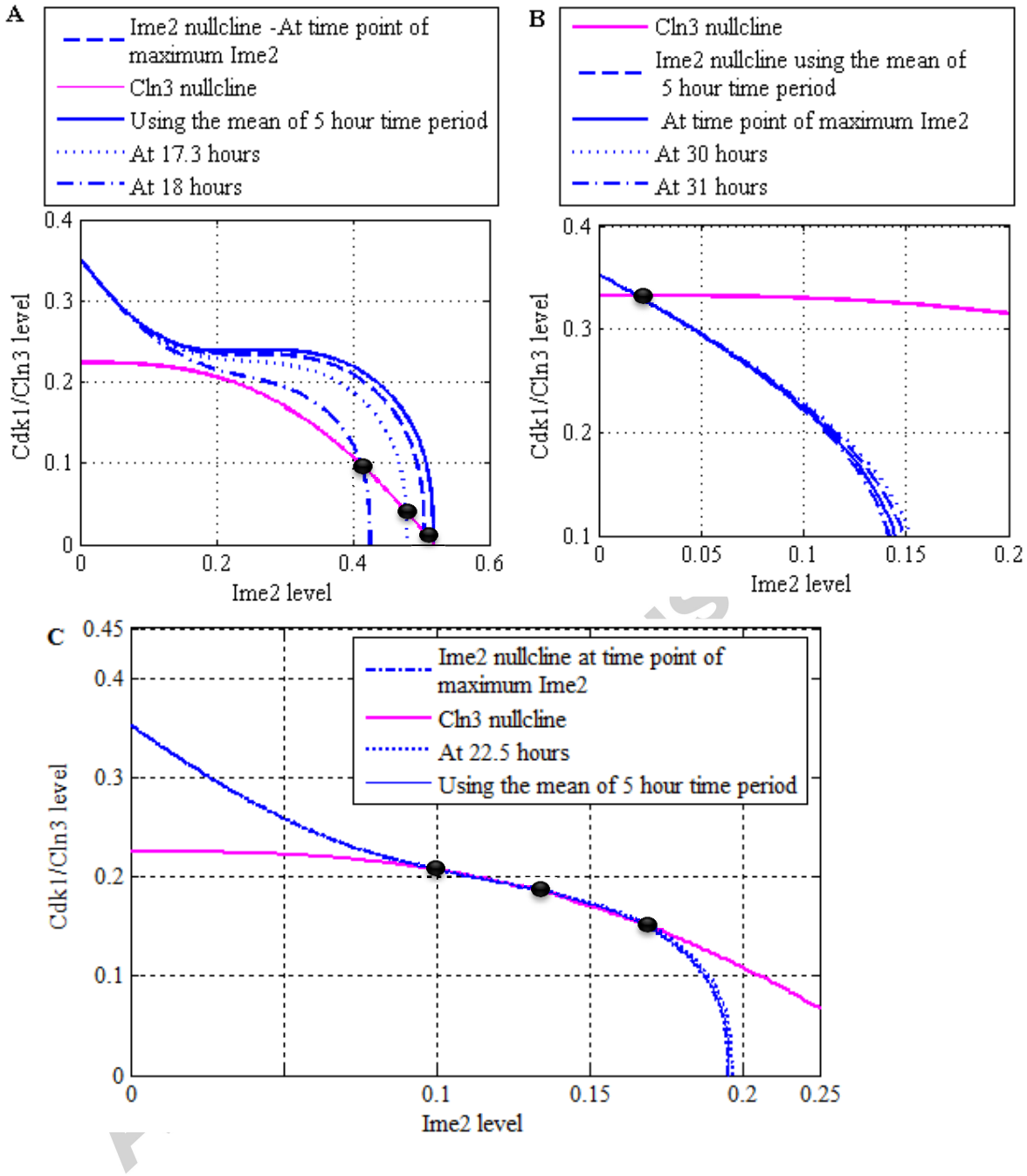

Figure 10

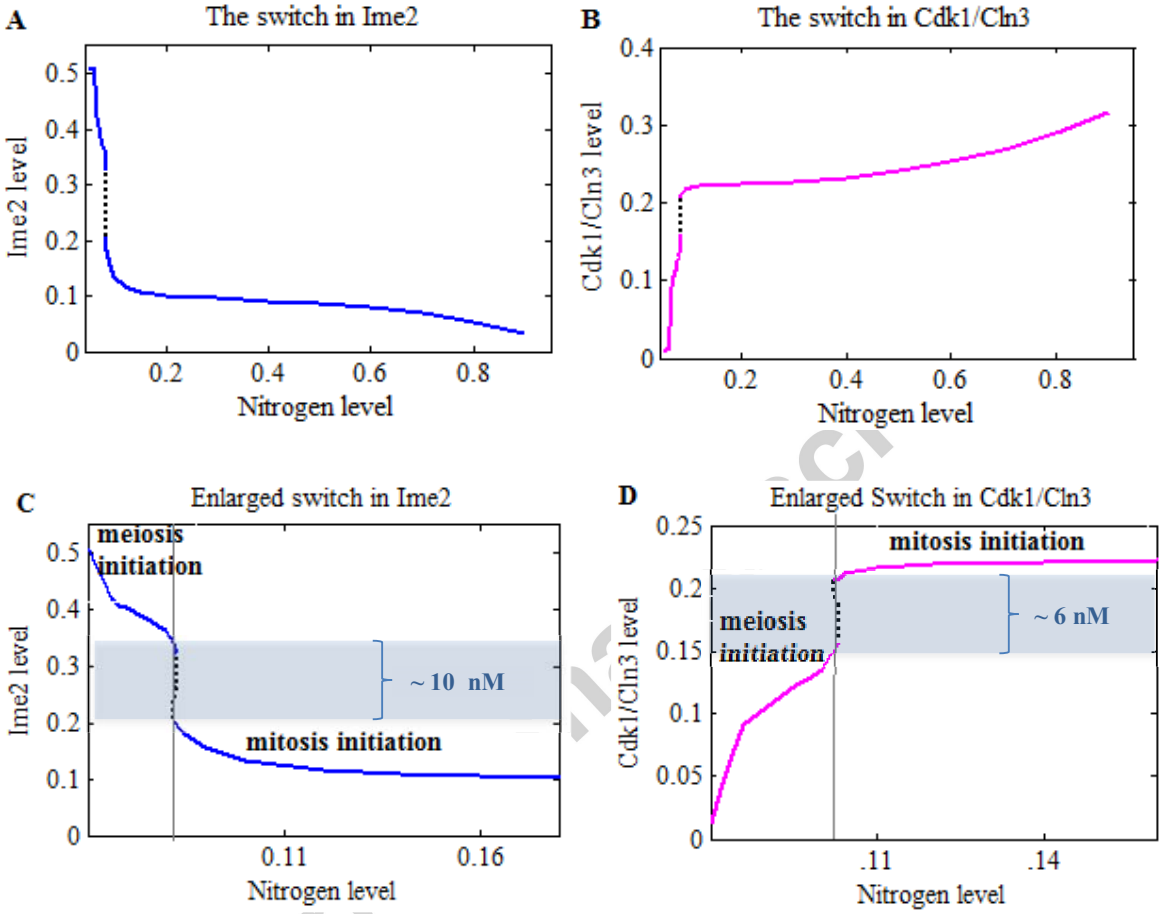

Figure 11